Electronic Supplementary Material (ESI) for Nanoscale.
This journal is © The Royal Society of Chemistry 2021

Graphene nanogaps for the directed assembly of single-nanoparticle devices

Electronic Supplementary Information

J. J. Cully[1], J. L. Swett[1], K. Willick[2], J. Baugh[2], and J. A. Mol*[3]

[1]Department of Computer Science, University of Oxford, UK
[2]Institute for Quantum Computing, University of Waterloo, Canada
[3]Department of Physics, Queen Mary University of London, UK

February 2021

*j.mol@qmul.ac.uk

1 The Simmons Model

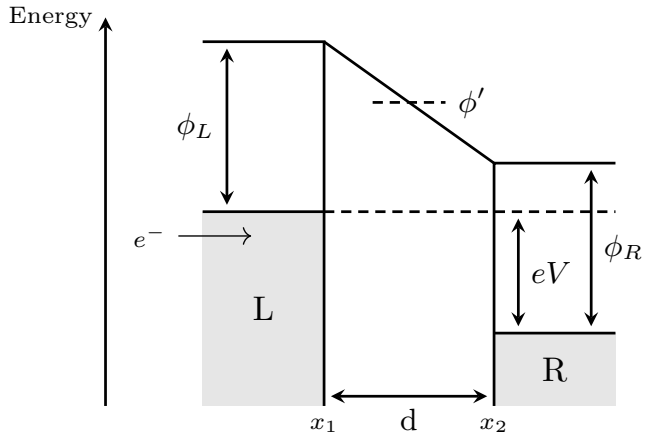

Figure S1: A trapezoidal tunnel barrier between a Left (L) and Right (R) electrode, separated by a distance d and an electrical bias V. Here, L and R are of the same material and at zero bias $\phi_L = \phi_R$.

An expression for the current density j flowing through a trapezoidal tunnel barrier of width $d = x_2 - x_1$ between two biased electrodes was derived by Simmons:[1]

$$j = e\frac{4\pi m}{h^3}\int_0^\infty d\epsilon[f_L(\epsilon) - f_R(\epsilon)]\int_0^\epsilon d\epsilon_x T(\epsilon_x) \tag{S1}$$

where m is the electron mass, $f_{L,R}(\epsilon) = (e^{-(\epsilon-\mu_{L,R})/k_BT} + 1)^{-1}$ is the Fermi energy of the left and right leads, respectively, dependent on their chemical potential $\mu_{L,R}$, and $T(\epsilon_x)$ describes the transmission probability of an electron of energy ϵ_x through the tunnel barrier in the x-direction. An expression for $T(\epsilon_x)$ can be found by using the Wentzel-Kramers-Brillouin (WKB) approximation:

$$T(\epsilon_x) = e^{-\beta\int_{x_1}^{x_2} dx\sqrt{\phi(x)-\epsilon_x}} \tag{S2}$$

where $\beta = 2\frac{\sqrt{2m}}{\hbar}$ and ϕ. If the work functions of the left and right leads are not equal, but change linearly from ϕ_L at x_1 to ϕ_R at x_2 as the a voltage V is applied symmetrically across the junction then we can write:

$$\phi_{L,R} = (1 \pm \alpha)\phi' \tag{S3}$$

where $\phi' = \frac{\phi_L-\phi_R}{2}$ is the average barrier height and $\alpha = \frac{\phi_L-\phi_R}{\phi_L+\phi_R}$ is an asymmetry factor, which are used for simplified fitting. Different analytical expressions for the integral $\int_{x_1}^{x_2} dx\sqrt{\phi(x)-\epsilon_x}$ can be found depending on the relative magnitudes of ϕ_L, ϕ_R and ϵ_x:[2]

$$\text{if } \phi_{\mathrm{L,R}} < \epsilon_{\mathrm{x}} < \phi_{\mathrm{R,L}} : \int_{\mathrm{x_1}}^{\mathrm{x_2}} \mathrm{dx}\sqrt{\phi(\mathrm{x}) - \epsilon_{\mathrm{x}}} = \mathrm{d}\frac{2}{3}\frac{(\phi_{\mathrm{R,L}} - \epsilon_{\mathrm{x}})^{3/2}}{\phi_{\mathrm{R}} - \phi_{\mathrm{L}}} \tag{S4}$$

$$\text{else } \epsilon_{\mathrm{x}} < \phi_{\mathrm{L}}, \phi_{\mathrm{R}} : \int_{\mathrm{x_1}}^{\mathrm{x_2}} \mathrm{dx}\sqrt{\phi(\mathrm{x}) - \epsilon_{\mathrm{x}}} = \mathrm{d}\frac{2}{3}\frac{(\phi_{\mathrm{R}} - \epsilon_{\mathrm{x}})^{3/2} - (\phi_{\mathrm{L}} - \epsilon_{\mathrm{x}})^{3/2}}{\phi_{\mathrm{R}} - \phi_{\mathrm{L}}} \tag{S5}$$

In the low temperature limit where $k_B T << \mu_L, \mu_R, \phi(x)$ the Fermi distribution becomes a step function and (S1) becomes:

$$j = e\frac{4\pi m}{h^3}\int_{\mu_R}^{\mu_L} d\epsilon \int_0^{\epsilon} d\epsilon_x T(\epsilon_x) \tag{S6}$$

In order to fit (S6) to the measured current I we must multiply it by the cross sectional area A' of the junction such that $I = A'j$. However, A' is not independent of other variables such as the effective electron mass and so is incorporated into a prefactor $A = e\frac{4\pi m}{h^3}A'$. Current-voltage data can then be fitted to the model to (S7) to find ϕ' [eV], α, d [m] and A [eV^{-2}].

$$I = A\int_{\mu_R}^{\mu_L} d\epsilon \int_0^{\epsilon} d\epsilon_x T(\epsilon_x) \tag{S7}$$

2 The Orthodox Model

Electron transport through a mesoscopic island separated by two tunnel barriers is well described by the classical 'orthodox' theory of correlated electron tunneling.[3–5] This model does not consider any discreteness of the energy spectrum of the island. This is a particularly good approximation for metals where level spacing is negligible. The orthodox theory can be extended to consider the presence of quantised energy levels provided that $k_B T$ is much greater than the intrinsic width of these levels, details of which can be found in[6,7], but this will not be considered here.

Figure S2 shows an equivalent 2-terminal RC circuit model that the orthodox theory describes. The tunnel rates $\Gamma_{L,R}^{+,-}$ capture the rate at which electrons are added to/taken off the island from to/from the left/right electrodes, as indicated by the arrows. We can describe the associated addition/subtraction energies with each added/removed electron starting from an initial state of n electrons on the island as:

$$\Delta E_{\mathrm{L}}^{+}(n) = U(n+1) - U(n) + \eta e V_b \tag{S8}$$

$$\Delta E_{\mathrm{L}}^{-}(n) = U(n) - U(n-1) + \eta e V_b \tag{S9}$$

$$\Delta E_{\mathrm{R}}^{+}(n) = U(n+1) - U(n) - (1-\eta) e V_b \tag{S10}$$

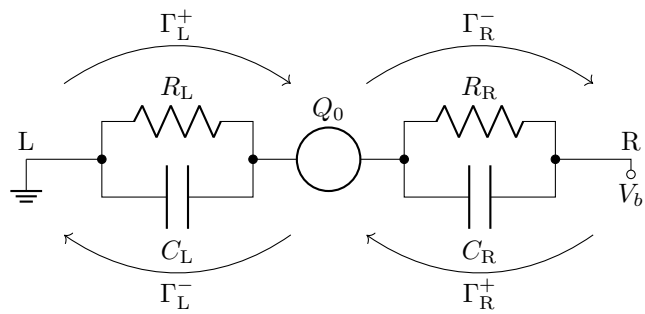

Figure S2: A circuit diagram representing the orthodox model. Each tunnel barrier is represented by a RC circuit and electrons tunnel from $(-)$/to $(+)$ the Left/Right electrodes at rate Γ. The central island has a residual fractional charge Q_0.

$$\Delta E_{\mathrm{R}}^{-}(n) = U(n) - U(n-1) - (1-\eta)eV_b \tag{S11}$$

Where $U(n)$ is the total energy of the island with n electrons, V_b is the bias voltage and η is the fraction of the voltage dropped over the left tunnel barrier. Within the limits of the model we can equivalently express these in electrostatic terms:

$$\Delta E_{\mathrm{L}}^{\pm}(n) = \Delta U^{\pm}(n) \pm \frac{eC_{\mathrm{R}}}{C_L + C_R} V_b \tag{S12}$$

$$\Delta E_{\mathrm{R}}^{\pm}(n) = \Delta U^{\pm}(n) \mp \frac{eC_{\mathrm{L}}}{C_L + C_R} V_b \tag{S13}$$

$$\Delta U^{\pm}(n) = \frac{(Q \pm e)^2}{2(C_L + C_R)} - \frac{Q^2}{2(C_L + C_R)} \tag{S14}$$

Where $Q = (ne - Q_0)$ is the total charge of the island before the electron tunnels and Q_0 is the fractional charge ($|Q_0| < e/2$) present on the island at zero bias. We can then write:

$$\Delta E_{\mathrm{L}}^{\pm}(n) = \frac{e}{C_L + C_R}\left(\frac{e}{2} \pm ((ne - Q_0) + C_{\mathrm{R}}V_b)\right) \tag{S15}$$

$$\Delta E_{\mathrm{R}}^{\pm}(n) = \frac{e}{C_L + C_R}\left(\frac{e}{2} \pm ((ne - Q_0) - C_{\mathrm{L}}V_b)\right) \tag{S16}$$

The tunnelling rates across the left-side and right-side barriers can be obtained from a golden rule calculation[3]:

$$\Gamma_{L,R}^{\pm}(n) = \frac{1}{R_{L,R}e^2}\left(\frac{-\Delta E_{L,R}^{\pm}(n)}{1 - \exp\left(\Delta E_{L,R}^{\pm}(n)/k_B T\right)}\right) \tag{S17}$$

Where any dependence of $\Gamma^{\pm}_{L,R}$ on n itself has been neglected. The current through the island at a given bias voltage is then given by:

$$I(V_b) = e \sum_{n=-\infty}^{\infty} \sigma(n) \left[\Gamma^{+}_{\mathrm{R}}(n) - \Gamma^{-}_{\mathrm{R}}(n)\right] = e \sum_{n=-\infty}^{\infty} \sigma(n) \left[\Gamma^{-}_{\mathrm{L}}(n) - \Gamma^{+}_{\mathrm{L}}(n)\right] \quad \text{(S18)}$$

Here, $\sigma(n)$ describes the ensemble distribution of the number of electrons on the island: the probability that any one value of n electrons are on the island. Finding $\sigma(n)$ requires noting that the net probability for making a transition between any two adjacent states is zero under a steady state, giving:

$$\sigma(n) \left[\Gamma^{+}_{\mathrm{L}}(n) + \Gamma^{+}_{\mathrm{R}}(n)\right] = \sigma(n+1) \left[\Gamma^{-}_{\mathrm{L}}(n+1) + \Gamma^{-}_{\mathrm{R}}(n+1)\right] \quad \text{(S19)}$$

and by implementing the normalisation condition $\sum_{n=-\infty}^{\infty} \sigma(n) = 1$. Thus, we can solve for $\sigma(n)$ and thereby $I(V_b)$ numerically.

We can extend this theory to include the influence of a gate electrode at voltage V_g connected to the island by a capacitor C_G by modifying (S15) and (S16) to:

$$\Delta E^{\pm}_{\mathrm{L}}(n) = \frac{e}{C_{\Sigma}} \left(\frac{e}{2} \pm ((ne - Q_0) + C_{\mathrm{R}} V_b - C_{\mathrm{G}} V_g)\right) \quad \text{(S20)}$$

$$\Delta E^{\pm}_{\mathrm{R}}(n) = \frac{e}{C_{\Sigma}} \left(\frac{e}{2} \pm ((ne - Q_0) - (C_{\mathrm{L}} + C_{\mathrm{G}}) V_b - C_{\mathrm{G}} V_g)\right) \quad \text{(S21)}$$

where $C_{\Sigma} = C_L + C_R + C_G$. From here the derivation of the current follows the same process as above.

3 Thermally Broadened Peaks

From Beenakker,[7] in the classical limit of $h\Gamma, \Delta E \ll k_B T \ll e^2/CE$ the lineshape of the Coulomb blockade resonances is given by:

$$G/G_{max} \approx \cosh^{-2}\left(\frac{\beta e |V_g - V_0|}{2.5 k_B T}\right) \quad \text{(S22)}$$

where β is the capacitive coupling to the gate, V_g is the gate voltage and V_0 is the voltage at which the resonance is centred.

4 Electric Field Calculations

The electric field distribution in our graphene devices was modelled using the finite element method in COMSOL Multiphysics 5.5 using the electric currents interface from the AC/DC physics module which computes electric fields and

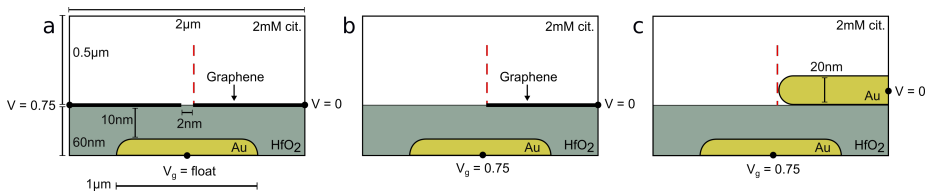

Figure S3: Schematics of the geometries used for electric field calculations for: (a) A 2 nm graphene nanogap with a floating buried gate, (b) a single graphene electrode trapping against a buried gate and (c) a 20 nm gold electrode trapping against a buried gate.

potential distributions for conducting media where inductive effects can be neglected. The model was solved in the frequency domain at $\omega = 1$ MHz. In this interface Poisson's equation is expressed as:

$$\nabla \cdot \mathbf{J} = Q = -\partial\rho/\partial t \tag{S23}$$

$$\mathbf{J} = \sigma\mathbf{E} + j\omega\mathbf{D} \tag{S24}$$

$$\mathbf{E} = -\nabla\varphi \tag{S25}$$

The simulation domain was built as shown in Figure S3a. The citrate solution was assumed to have a permittivity of 80 and was found to have a conductivity of $600\,\mu\mathrm{S\,cm^{-1}}$. The HfO_2 was assigned a permittivity of 13 [8] and a negligible conductivity. Dirichlet boundary conditions of $\varphi = 0.75$ and $\varphi = 0$ were set on the left and right vertices of the graphene layer at the edges of the simulation domain, respectively. The buried gate electrode was assigned a 'floating potential' boundary condition. All other external boundaries were set to an insulating Neumann boundary condition $\mathbf{n} \cdot \mathbf{J} = 0$. At the graphene layer a dielectric shielding boundary condition was used whereby:

$$\mathbf{n} \cdot (\mathbf{J}_1 - \mathbf{J}_2) = -\nabla_T \cdot d_s d((\sigma + j\omega\varepsilon_0\varepsilon_r)\nabla_T\varphi) \tag{S26}$$

where $\mathbf{n}$ is the normal vector, $\mathbf{J}_{1,2}$ are the current densities on either side of the boundary, ∇_T is the tangential differential, d_s is the thickness of the boundary which was set as 1 nm. We used $\varepsilon_r = 6.9$ [9] and set the conductivity as $\sigma = e\mu_e\, n_{2D}(\varphi(x))$, where μ_e is the electron mobility in graphene (2.5×10^4 $\mathrm{cm^2V^{-1}s^{-1}}$ [10]) and n_{2D} is the surface charge concentration per unit area. This was defined according to the analytical expression presented by Barik *et al.*:[11]

$$n_{2D}(\varphi(x)) = 2\frac{\Gamma(2)}{\pi}\left(\frac{k_B T}{\hbar\nu_F}\right)^2 \left[\mathcal{F}_1(\frac{e\varphi(x)}{k_B T}) - \mathcal{F}_1(\frac{-e\varphi(x)}{k_B T})\right] \tag{S27}$$

where ν_F is the Fermi velocity (10^6 ms^{-1} in graphene), $\varphi(x)$ is the electric potential at position x in the graphene layer and $\mathcal{F}_1$ is the Fermi-Dirac integral of order 1:

$$\mathcal{F}_j = \frac{1}{\Gamma(j+1)} \int_0^\infty \frac{\epsilon^j \, d\epsilon}{e^{\epsilon-\eta}+1} \tag{S28}$$

where $\eta = \pm/k_B T$ and $\Gamma(n) = (n-1)!$. $n_{2D}(x)$ was calculated in MATLAB using the algorithm published by Wang and Lundstrom,[12] which was then used by COMSOL in a self-consistent calculation for φ.

The calculations for a single graphene electrode trapping against a local gate electrode were configured in much the same way, except that the gate electrode was assigned a Dirichlet boundary condition of $\varphi = V_g = 0.75$ and the left electrode was removed. This is shown in Figure S3b. For the gold electrode a 20 nm high, rounded geometry was used, and the potential difference was again applied between the buried gate and the right electrode as shown in Figure S3c. The gold was assigned a conductivity of $4.6 \times 10^7\,\mathrm{S\,cm^{-1}}$ [13] and a permittivity of 1.

References

[1] J. G. Simmons, *J. Appl. Phys.*, 1963, **34**, 1793–1803.

[2] F. Prins, A. Barreiro, J. W. Ruitenberg, J. S. Seldenthuis, N. Aliaga-Alcalde, L. M. K. Vandersypen and H. S. J. van der Zant, *Nano Lett.*, 2011, **11**, 4607–4611.

[3] D. Averin and K. Likharev, *Mesoscopic Phenom. Solids*, Elsevier, New York, 1991, ch. 6, pp. 173–271.

[4] M. Amman, R. Wilkins, E. Ben-Jacob, P. D. Maker and R. C. Jaklevic, *Phys. Rev. B*, 1991, **43**, 1146–1149.

[5] A. E. Hanna and M. Tinkham, *Phys. Rev. B*, 1991, **44**, 5919–5922.

[6] E. B. Foxman, P. L. McEuen, U. Meirav, N. S. Wingreen, Y. Meir, P. A. Belk, N. R. Belk, M. A. Kastner and S. J. Wind, *Phys. Rev. B*, 1993, **47**, 10020–10023.

[7] C. W. Beenakker, *Phys. Rev. B*, 1991, **44**, 1646–1656.

[8] B. Lee, T. Moon, T.-G. Kim, D.-K. Choi and B. Park, *Appl. Phys. Lett.*, 2005, **87**, 012901.

[9] Y. Wu, Y. Xu, Z. Wang, C. Xu, Z. Tang, Y. Chen and R. Xu, *Appl. Phys. Lett.*, 2012, **101**, 99–102.

[10] K. Bolotin, K. Sikes, Z. Jiang, M. Klima, G. Fudenberg, J. Hone, P. Kim and H. Stormer, *Solid State Commun.*, 2008, **146**, 351–355.

[11] A. Barik, Y. Zhang, R. Grassi, B. P. Nadappuram, J. B. Edel, T. Low, S. J. Koester and S.-H. Oh, *Nat. Commun.*, 2017, **8**, 1867.

[12] X. Wang and M. Lundstrom, *Fermi-Dirac integral using a table method in MATLAB*, 2019, https://github.com/wang159/FDIntegral_Table.

[13] C. Kittel, *Introduction to Solid State Physics*, Wiley, New York, 7th edn, 1996, p. 150.